ANALYTICAL MODELING OF SATELLITES IN GEOSYNCHRONOUS ENVIRONMENT

N. John Stevens
NASA Lewis Research Center

SUMMARY

Geosynchronous satellites are known to be charged by the geomagnetic substorm environment. Surface charging is often sufficient to result in discharges that can couple transients into satellite electrical harnesses and produce electronic upsets in systems. Ground simulation testing of surface charging has been and is being conducted by using monoenergetic electron beams. Results have shown that massive discharges on dielectric surfaces could occur with sufficiently large differential voltages between the surface and the substrate. With the advent of three-dimensional analytical modeling techniques, however, it has become apparent that the large differential voltages required for these massive laboratory discharges do not occur on satellites in space. The modeling predictions are supported by dielectric charging data from P78-2, SCATHA (Spacecraft Charging at High Altitudes) flight results. Hence other mechanisms leading to discharges on satellite surfaces must be found. Three such mechanisms discussed in this paper are ungrounded insulator areas, buried charge layers (due to mid-energy-range particles), and positive differential voltages (where structure voltages are less negative than surrounding dielectric surface voltages).

INTRODUCTION

In the early 1970's, it was found that the Applications Technology Satellite 5 (ATS-5) spacecraft potential was driven to significant negative voltages when the satellite was in the local midnight region of its orbit (refs. 1 to 4). Values extending to -10 000 volts when the satellite experienced the spring and fall eclipse periods and to -300 volts when the satellite was in sunlight were observed (refs. 2 and 5). The cause of this charging was found to be magnetospheric plasma clouds (substorms) that are periodically generated in this midnight region. The differences in potential between eclipse and sunlight charging events were due to photoemission from sunlit surfaces.

Although this phenomenon was of interest, it was not believed to be serious for system operations since it did not seem to cause problems. When a Defense Satellite Communications System (DSCS) II satellite system failed in 1973, however, the failure review started locating numerous instances of electronic switching anomalies in DSCS II and other geosynchronous satellites (ref. 6). When these anomalous switching events were plotted against local time of occurrence, a peculiar pattern developed (fig. 1). The radial separation of the anomaly distribution in this figure has no significance; it is simply a means of separating the occurrences. The bars indicate the uncertainty in the time of occurrence. From this figure it is apparent that anomalies occurred in the midnight to dawn segment of the orbit, implying substorm charging events.

When the ATS-6 spacecraft was launched in 1974, charging was again observed. Ground potentials on the satellite were driven to -2.2 kilovolts during sunlight charging and to -19 kilovolts during eclipse charging (maximum potentials reported in refs. 4 and 7). Much care was taken to make this satellite immune to external radiation since it had to operate in its own radiofrequency (rf) beam. As a result of this careful design the substorm charging phenomenon did not cause any system upsets (ref. 8). The data from this satellite indicated that spacecraft charging could be related to the absence of low-energy plasmas (fig. 2, ref. 7). Apparently the substorm has the effect of suppressing the natural environment, low-energy plasma.

In 1975, a cooperative Air Force and NASA spacecraft charging investigation was begun to develop means of controlling the absolute and differential charging of geosynchronous satellite surfaces by geomagnetic substorm environments (ref. 9). Although there had been only one catastrophic failure of a satellite system, it was felt that the charging and discharging cycles could have a detrimental effect on future, long-life, unattended-operation missions that were being proposed. Therefore the investigation of this phenomenon and its effect on satellite systems was a logical candidate for a technology program.

The ground technology program concentrated on developing analytical tools and conducting ground simulation experiments in support of the P78-2 (Spacecraft Charging at High Altitudes (SCATHA)) flight program. Both ground technology and flight data were necessary to produce the design guidelines, environmental atlas, and test standards required as the output of the cooperative investigation.

Ground simulation testing was begun first. Monoenergetic electron beams were used to charge typical spacecraft dielectric samples. The responses of the dielectrics were carefully measured and evaluated (ref. 10). When breakdown voltage thresholds were exceeded, discharges occurred and produced spectacular, lightning-like displays (fig. 3). These studies indicated that surface charging could be explained in terms of current balances (ref. 11) and that a differential voltage between the dielectric surface and substrate of 8 to 15 kilovolts was required for discharges.

When discharges did occur, it was found that the energy lost from the sample was large and scaled with the square root of the sample area (refs. 12 and 13). The significant results, characterized in table I, were consistent with the prevailing concepts of spacecraft charging interactions. On the basis of ATS-5/6 data, it was felt that large differential voltages between dielectric surfaces and the subsurface could be developed by substorm encounters.

The development of modeling tools has been proceeding slowly since the start of the joint investigation. The NASA Charging Analyzer Program (NASCAP) has now reached a stage where its predictive capability has been sufficiently cross-checked against ground simulation and flight data (refs. 14 to 17). Computation of satellite behavior in actual space environments indicates that some of the original charging concepts are in error and should be reviewed.

This paper reviews the modeling computations and discusses the effect on discharge processes.

SYMBOLS

A	area
C	capacitance
E_m	mid-energy-range incident electron
I	current
n_e	electron number density
n_p	proton number density
P	incident particles (electrons and protons)
P_o	photoemitted electrons
s	secondary emitted electrons
T_e	electron temperature
T_p	proton temperature
V_L	voltage at buried charge layer in dielectric
V_S	dielectric surface voltage
$V_{S/C}$	spacecraft structure voltage

GEOSYNCHRONOUS SATELLITE MODELING

The behavior of geosynchronous satellites in space environments was analyzed by using the NASCAP computer code, a three-dimensional code capable of predicting the response of satellite surfaces to a specified environmental flux as a function of time. The code considers the material properties (e.g., bulk and surface conduction, secondary emission, backscatter, and photoemission) and the influence of fields generated around the satellite by the charged surfaces in computing surface voltages. The code has been described in the literature (refs. 18 to 20).

The satellite model used in NASCAP is shown in figure 4. This model represents a typical three-axis-stabilized satellite as used in the late 1970's. It has two large solar array wings that are assumed to be Sun oriented and capable of generating about a kilowatt of power. It is assumed that the arrays function at 50 volts when generating power. The Sun-facing surface of the array has a silica cover glass that is coated with a magnesium fluoride antireflective coating. The array is assumed to have a 4-mil-thick Kapton substrate. The interconnections are modeled as patches on the array

(to simulate the total interconnection area) and are assumed to be an oxidized aluminum surface. The body of the satellite has Earth-facing antennas and a rear thruster chamber. The body is covered with various dielectrics as shown.

Environmental conditions used in this analysis consist of single Maxwellian temperatures for electrons (with proton temperatures assumed to be twice the electron temperatures), and equal electron and proton densities. Sunlight (with Sun incidence at 27°) and eclipse conditions were used in this analysis.

The predicted surface potentials (relative to space plasma potential) are shown for selected surfaces, as a function of time, in figure 5. In the first 1000 seconds, when substorm conditions are characterized by 3-keV electron temperatures, no appreciable charging occurs. The concept that a threshold particle temperature must be reached before charging can begin is seen to apply (ref. 21). In the next 1000-second interval, with the satellite still in sunlight but with the substorm intensity increased to 8-keV electron temperatures, both absolute charging and differential charging occur. Differential charging here is defined as the difference between the dielectric surface voltage and the spacecraft structure. Note that the shaded Kapton has become more negative than the spacecraft structure (satellite electrical ground) and that the solar array cover glass is positive with respect to the structure.

When the satellite enters eclipse, there is a rapid change in absolute charging followed by a slower development in differential charging. This is consistent with ground results on charging rates (ref. 22) and has been shown to be true for both 8- and 12-keV substorms. Note that the differential charging of the solar array covers has become more positive with respect to the structure but that the shaded insulators have become more negative. Upon entering the sunlight again, there is another rapid change in absolute values followed by a slower readjustment of differential voltages. Finally, in the last 2000 seconds of this analysis, substorm conditions are allowed to become progressively less intense, and the spacecraft potentials relax accordingly.

This analysis predicts two effects that were not anticipated:

(1) Low differential voltages across the shaded insulators

(2) Positive differential voltages on the solar array

The maximum differential voltage across the 4-mil-thick Kapton used in this study is only about 2 kilovolts. Analyses of different satellites under different environmental conditions indicate that, while the absolute voltages can be shifted, the differential voltages remain about the same; that is, the maximum differential voltages across shaded insulators are never predicted to be greater than 4 kilovolts (refs. 23 to 27). This result is due to the suppression of photo- and secondary emission by the three-dimensional electric fields developed on the more negatively charged surfaces (ref. 28). This predicted low level of differential voltage agrees with the P78-2 (SCATHA) surface potential monitor data. Ungrounded spot voltages measured by this monitor indicated differential values reaching -2 kilovolts even though the structure potential reached values to -8 kilovolts relative to the space plasma potential (ref. 29).

The positive differential voltages predicted for solar array cover glasses can range from a few volts to kilovolts depending on the secondary emission characteristics assumed for coatings applied to these covers. For reasonable ranges of values the differential voltage across the cover glass is always positive (refs. 23 to 27). Ground simulation testing is usually conducted by grounding the array electrical circuit and irradiating the cover glass with monoenergetic electrons (ref. 10). Doing so results in a negative differential voltage cross the cover glass; that is, cover glass surface voltages are strongly negative with respect to the grounded electrical circuit.

According to the analytical results predicted in this study, discharges similar to those observed in the laboratory should not occur on satellites. The differential voltage across shaded insulators is predicted to be too low to exceed the breakdown threshold derived from ground tests, and the predicted differential voltage across the solar array cover glass is the wrong polarity as compared with the ground test conditions. Yet the fact remains that discharges do occur on satellites (refs. 30 and 31). Therefore it becomes necessary to investigate other possible means of producing discharges in a space environment.

DISCHARGE MECHANISMS

From the preceding discussion it is apparent that the mechanisms leading to satellite discharges are not the same as those studied in the laboratory. Three mechanisms leading to discharges are possible:

(1) Ungrounded insulators
(2) Buried or trapped charge layers
(3) Positive differential voltages

These mechanisms are discussed in this section.

Ungrounded Insulators

Dielectric areas electrically decoupled from the satellite can charge much more rapidly than areas that remain coupled. Decoupling can occur by breaking electrical grounds to the metallic areas of thermal blankets or optical solar reflectors (OSR). Figure 6 shows a comparison of predicted surface voltages for shaded Kapton and OSR regions in a 8-keV electron temperature substorm. Figure 6(a) shows voltage predictions when these regions are coupled (i.e., metallic areas grounded to structure). Both absolute charging and differential charging are seen to develop slowly. Figure 6(b) shows the voltage predictions with the grounds broken and the insulator regions capacitively coupled to the structure with a capacitance of 10^{-12} farad. Differential charging of these regions occurs rapidly while the structure slowly charges. In this case a large differential voltage can occur in seconds. However, it should be pointed out that the energy storage (for possible discharge pulses) is low because of the small capacitance. The differential voltages for ungrounded insulators could be larger than the 2 kilovolts obtained in this example if different materials and environments were used. Although this type of charging mechanism is always possible, it may develop with time in orbit as a result of the breakup of the thin vapor deposited metal used on these insulators. Hence it is difficult to predict and the only means of protection would be to give careful attention to grounding.

Buried or Trapped Charge Layers

Ground testing of dielectrics with low-energy, monoenergetic electrons (0 to 20 keV) results in charges being deposited on or near the exposed dielectric surface. These incoming (primary) electrons generate secondary electrons, and eventually an equilibrium is reached. The surface is at a characteristic voltage such that the net current to that surface is zero. However, if the electron energies are higher (100 keV), the incoming particles penetrate the surface and become buried within the dielectric or possibly pass completely through and thus produce different surface voltage characteristics than in the low-energy case. If a test were run in an environment combining a relatively high flux of low-energy electrons (e.g., 5 keV) with a lower flux of mid-energy electrons (e.g., 50 keV), one would expect the dielectric surface to respond to the low-energy flux by developing a characteristic voltage and the mid-energy electrons to penetrate the surface and be buried (fig. 7). A low differential voltage would thus occur between the dielectric surface and the substrate, but very strong voltage gradients would occur within the dielectric because of the buried charges. These gradients could be sufficient to trigger discharges.

In space there is a wide distribution of particle energies. Data on the substorm environment from the P78-2 (SCATHA) instruments (ref. 32) indicate that there is a large constituent of electrons in the mid-energy range (100 keV). In addition, there is a significant ion flux distributed over a wide energy range. Under these conditions it could be possible to duplicate the combined-flux test just described. The low-energy component of the electron flux and the ion flux would interact with the satellite surfaces to produce a relatively low negative surface voltage (the electron flux dominating). If the surface were in sunlight, photoemission from the surface would reduce the negative surface voltage. The mid-energy component of substorm electrons could be buried within the satellite surfaces and generate strong voltage gradients that could trigger discharges. Edges and imperfections in the dielectric can enhance the probability of discharge. NASCAP modeling of satellite behavior does not treat the concept of buried charge, and so would not be able to predict anything other than the surface voltage.

This concept of buried charge was proposed several years ago (ref. 33) and is currently being evaluated analytically (ref. 34) and experimentally (ref. 35). A criterion for breakdown found in the experimental work is a gradient in excess of 2×10^5 volts per centimeter. Although this mechanism appears to be a logical means of producing discharges in satellites, additional studies must be conducted.

A phenomenon that might be related to this proposed trapped-charge mechanism is a discharge that is generated in low-energy-electron-beam ground tests. This type of discharge, which occurs infrequently but repeatedly when dielectrics have been differentially charged to a few kilovolts, is usually ignored because of the small resultant pulse and charge loss. In view of the low predicted differential voltages on satellites, however, these low-voltage discharges should be reevaluated.

Positive Differential Voltages

A positive differential voltage exists when the dielectric surface is at a less negative voltage than the substructure. If there are cracks, edges, or gaps that expose the substructure through the dielectric, a small "electron gun" exists, with the substructure forming a cathode and the dielectric the accelerator plates. Discharges are possible if the differential voltage becomes large enough.

As an example of this mechanism, consider the predicted differential voltages for the solar array on the model used in this study (fig. 8). The coverglass properties include a high-secondary-yield, magnesium fluoride antireflection coating commonly used on space solar arrays. A very strong positive differential voltage exists in the middle and outer areas of this array during the very intense phases of the substorm and is especially large in eclipse (1 kV). Studies of solar array segments with the electrical circuit biased to negative voltages while exposed to plasma environments have shown that breakdowns are possible (ref. 36). Since the laboratory breakdown phenomenon occurred under conditions analogous to those predicted here, it is conceivable that spacecraft discharges could result from this mechanism. Studies conducted with an electrically floating solar array irradiated by monoenergetic electrons have also indicated discharge patterns (ref. 37).

Although only solar arrays have been discussed herein, similar conditions are predicted to exist for dielectric booms on satellites (ref. 27). In either case it is important and necessary to pursue studies of this breakdown mechanism.

CONCLUDING REMARKS

Reviews of geosynchronous satellite data from ATS-5 to P78-2 (SCATHA) have indicated that satellite surfaces are charged by the geomagnetic environment, that discharges occur, that pulses from discharges can couple into spacecraft harnesses, and that electronic switching anomalies can result. Ground simulation testing has concentrated on discharge phenomena resulting from large differential voltages across dielectrics under the impression that large voltage differences were possible in space conditions. Such testing has resulted in cataloging the characteristics of large differential discharges.

Analytical modeling of satellites in geosynchronous environments with the NASCAP code has matured to a point where predictions agree with observed charging trends. The results of computations based on this modeling indicate that differential voltages on satellites are considerably smaller than those required to trigger discharges in ground tests, an indication that discharges on satellites in space are not the same as those studied in ground simulation tests. Therefore it became necessary to explore other mechanisms that could lead to discharges on satellites.

Three possible mechanisms are suggested in this report. The first is ungrounded insulators, where the dielectric is weakly capacitively coupled to the structure and can charge rapidly. The second is the buried charge layer,

where the mid-energy component of the electron flux in substorms can be buried or trapped within the dielectric, producing strong internal voltage gradients and possibly triggering discharges. The third is positive differential voltages, which can occur when the structure is more negative than the surrounding dielectric.

Each of these proposed mechanisms must be studied to determine if it could be responsible for the spacecraft charging type of discharges. To date, little work has been done on any of them. It is necessary to establish these discharge mechanisms consistent with ground tests, analysis, and space data in order to define a credible discharge criterion for designers to use.

REFERENCES

1. DeForest, S. E.; and McIlwain, C. E.: Plasma Clouds in the Magnetosphere. J. Geophys. Res., vol. 76, June 1971, pp. 3587-3611.
2. DeForest, S. E.: Spacecraft Charging at Synchronous Orbit. J. Geophys. Res., vol. 77, no. 2, Feb. 1972, pp. 651-659.
3. Fredericks, R. W.; and Scarf, F. L.: Observations of Spacecraft Charging Effects in Energetic Plasma Regions. Photon and Particle Interactions with Surfaces in Space, R. J. L. Grard, ed., Astrophysics and Space Science Library, Vol. 37, D. Reidel Publishing Co., 1973, pp. 277-308.
4. Bartlett, R. O; DeForest, S. E.; and Goldstein, R.: Spacecraft Charging Control Demonstration at Geosynchronous Altitude. AIAA Paper 75-359, Mar. 1975.
5. Rubin, A. G.; and Garrett, H. B.: ATS-5 and ATS-6 Potentials During Eclipse. Spacecraft Charging Technology - 1978, NASA CP-2071, AFGL TR-79-0082, 1979, pp. 38-43.
6. McPherson, D. A.; Cauffman, D. P.; and Schober, W.: Spacecraft Charging at the High Altitudes: The SCATHA Program. Spacecraft Charging by Magnetospheric Plasmas, A. Rosen, ed., Progress in Astronautics and Aeronautics, Vol. 47, American Institute of Aeronautics and Astronautics, Inc., 1976, pp. 15-30.
7. Reasoner, D. L.; Lennartsson, W.; and Chappel, C. R.: Relationship Between ATS-6 Spacecraft Charging Occurrences and Warm Plasma Encounters. Spacecraft Charging by Magnetospheric Plasmas, A. Rosen, ed., Progress in Astronautics and Aeronautics, Vol. 47, American Institute of Aeronautics and Astronautics, Inc., 1976, pp. 89-101.
8. Kampinsky, A.; and Keiser, B. E.: ATS-6 Spacecraft: An EMC Challenge," NASA TM X-70795, 1974.
9. Lovell, R. R.; et al.: Spacecraft Charging Investigation: A Joint Research and Technology Program. Spacecraft Charging by Magnetospheric Plasmas, A. Rosen, ed., Progress in Astronautics and Aeronautics, Vol. 47, American Institute of Aeronautics and Astronautics, Inc., 1976, pp. 3-14.
10. Materials Characterization papers in Proceedings of the Spacecraft Charging Technology Conference, R. P. Pike and R. R. Lovell, eds., AFGL TR-77-0051, NASA TM X-73537, 1977, pp. 431-547. Material Characterization papers in Spacecraft Charging Technology - 1978, NASA CP-2071, AFGL TR-79-0082, 1979, pp. 437-756.
11. Purvis, C. K.; Stevens, N. J.; and Oglebay, J. C.: Charging Characteristics of Materials: Comparison of Experimental Results with

Simple Analytical Models. Proceedings of the Spacecraft Charging Technology Conference, C. P. Pike and R. R. Lovell, eds., AFGL TR-77-0051, NASA TM X-73537, 1977, pp. 459-486.
12. Aron, P. R.; and Staskus, J. V.: Area Scaling Investigations of Charging Phenomena. Spacecraft Charging Technology - 1978, NASA CP-2071, AFGL TR-79-0082, 1979, pp. 485-506.
13. Balmain, K. G.: Scaling Laws and Edge Effects for Polymer Surface Discharges. Spacecraft Charging Technology - 1978, NASA CP-2071, AFGL TR-79-0082, 1979, pp. 646-656.
14. Stevens, N. J.; et al.: Initial Comparison of SSPM Ground Test Results and Flight Data to NASCAP Simulations. NASA TM-81394, 1980.
15. Schneulle, G. W.; et al.: Simulation of the Charging Response of the SCATHA (P78-2) Satellite. Spacecraft Charging Technology - 1980. NASA CP-2182, 1981.
16. Purvis, C. K.; and Staskus, J.: SSPM Charging Response: Comparison of Ground Test and Flight Data to NASCAP Predictions for Eclipse Conditions. Spacecraft Charging Technology - 1980. NASA CP-2182, 1981.
17. Saflekos, N. A.; et al.: Three Dimensional Analysis of Charging Events on Days 87 and 114, 1979, from SCATHA. Spacecraft Charging Technology - 1980. NASA CP-2182, 1981.
18. Katz, I.; et al.: A Three Dimensional Dynamic Study of Electrostatic Charging in Materials. (SSS-R-77-3367, Systems, Science and Software; NASA Contract NAS3-20119.) NASA CR-135256, 1977.
19. Katz, I.; et al.: Extension Validation and Application of the NASCAP Code. (SSS-R-79-3904, Systems, Science and Software; NASA Contract NAS3-21050.) NASA CR-159595, 1979.
20. Katz, I.; et al.: Capabilities of the NASA Charging Analyzer Program. Spacecraft Charging Technology - 1978, NASA CP-2071, AFGL TR-79-0082, 1979, pp. 101-122.
21. Garrett, H. B.; et al.: Comparison Between the 30-80 keV Electron Channels on ATS-6 and 1976-059A During Conjunction and Application to Spacecraft Charging Prediction. J. Geophys. Res., vol. 85, Mar. 1, 1980, pp. 1155-1162.
22. Purvis, C. K.; et al.: Charging Rates of Metal-Dielectric Structures. Spacecraft Charging Technology - 1978, NASA CP-2071, AFGL TR-79-0082, 1979, pp. 507-523.
23. Stevens, N. J.; and Roche, J. C.: NASCAP Modelling of Environmental-Charging-Induced Discharges in Satellites. NASA TM-79247, 1979.
24. Stevens, N. J.: Computed Voltage Distributions Around Solar Electric Propulsion Spacecraft," NASA TM-79286, 1979.
25. Stevens, N. J.; and Purvis, C. K.: NASCAP Modelling Computations on Large Optics Spacecraft in Geosynchronous Substorm Environments. Optics in Adverse Environments, Vol. 216. M. A. Kahan, ed., Society of Photo-Optical Instrumentation Engineers, 1980, pp. 116-130. (Also NASA TM-81395, 1980.)
26. Sanders, N. L., and Inouye, G. T.: NASCAP Charging Calculations for a Synchronous Orbit Satellite. Spacecraft Charging Technology - 1980. NASA CP-2182, 1981.
27. Stevens, N. J.: Utilization of Charging Control Guidelines in Geosynchrous Satellite Design Studies. Spacecraft Charging Technology - 1980. NASA CP-2182, 1981.

28. Mandell, M. J.; et al.: The Decrease in Effective Photocurrents Due to Saddle Points in Electrostatic Potentials Near Differentially Charged Spacecraft. IEEE Trans. Nucl. Sci., vol. NS-25, no. 6, Dec. 1978, pp. 1313-1317.
29. Mizera, P. M.; and Fennell, J. F.: Satellite Surface Potential Survey. Spacecraft Charging Technology - 1980. NASA CP-2182, 1981.
30. Damron, S. A.; Adam, R. C.; and Nanevicz, J. E.: Transient Pulse Monitor (TPM) Data from the SCATHA/P78-2 Spacecraft. Spacecraft Charging Technology - 1980. NASA CP-2182, 1981.
31. Koons, H. C.: Aspect Dependence and Frequency Spectrum of Electrical Discharges on the P78-2 (SCATHA) Satellite. Spacecraft Charging Technology - 1980. NASA CP-2182, 1981.
32. Reagan, J. B.; et al.: The Role of Energetic Electrons in Charging/ Discharging of Spacecraft Dielectrics. Spacecraft Charging Technology - 1980. NASA CP-2182, 1981.
33. Meulenberg, A., Jr.: Evidence for a New Discharge Mechanism for Dielectrics in a Plasma. Spacecraft Charging by Magnetospheric Plasmas, A. Rosen ed., Progress in Astronautics and Aeronautics, Vol. 47, American Institute of Aeronautics and Astronautics, Inc., 1976, pp. 237-246.
34. Beers, B. L.; and Pine, V. W.: Electron Beam Charged Dielectrics - Internal Charge Distribution. Spacecraft Charging Technology - 1980. NASA CP-2182, 1981.
35. Frederickson, A. R.: Bulk Charging and Discharging Characteristics of Several Polymers. Spacecraft Charging Technology - 1980. NASA CP-2182, 1981.
36. Stevens, N. J.: Space Environmental Interactions with Biased Spacecraft Surfaces. Space Systems and Their Interactions with Earth's Space Environment, H. B. Garrett and C. P. Pike, eds., Progress in Astronautics and Aeronautics, Vol. 71, American Institute of Aeronautics and Astronautics, Inc., 1980, pp. 455-476.
37. Inouye, G. W.; and Sellen, J. M., Jr.: TDRSS Solar Array Arc Discharge Tests. Spacecraft Charging Technology - 1978, NASA CP-2071, AFGL TR-79-0082, 1979, pp. 834-852.

TABLE I. - TYPICAL DISCHARGE CHARACTERISTICS

[Ground simulation test.]

Breakdown thresholds:	
Dielectric punchthrough, V/cm (kV/mil)	3×10^6 (7)
Edge breakdown, V/cm (kV/mil):	
Teflon and Kapton	$\sim10^6$ (3)
Solar cells	$\sim4\times10^5$ (1)
Area scaling for discharges:	
Return current amplitude	$I \propto A^{1/2}$
Pulse duration	$I \propto A^{1/2}$
Discharge propagation velocity, cm/sec	2×10^7

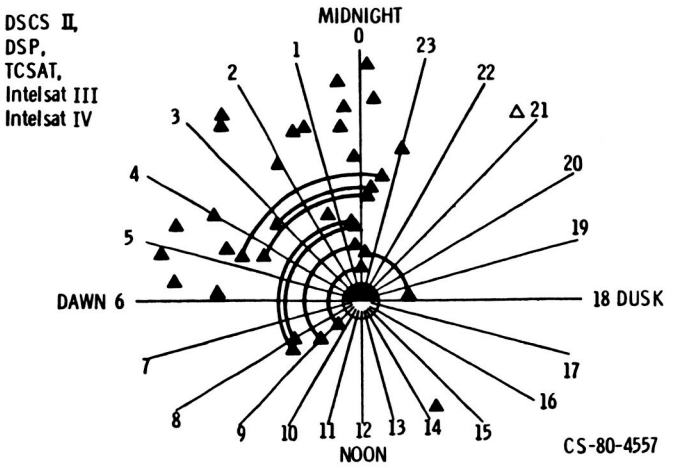

Figure 1. - Occurrence of satellite anomalies in local time.

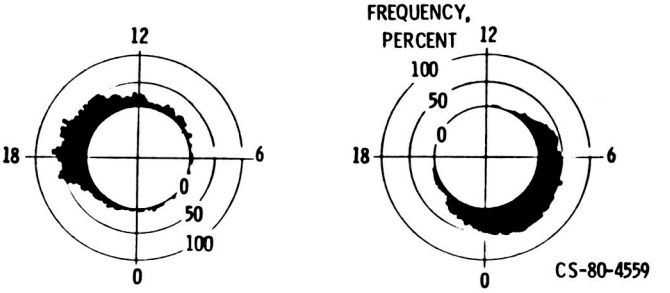

(a) Low-energy plasma encounter.

(b) Spacecraft charging events.

Figure 2. - ATS-6 environment data - local time distributions.

Figure 3. - Discharges in single-sheet silvered Teflon sample.

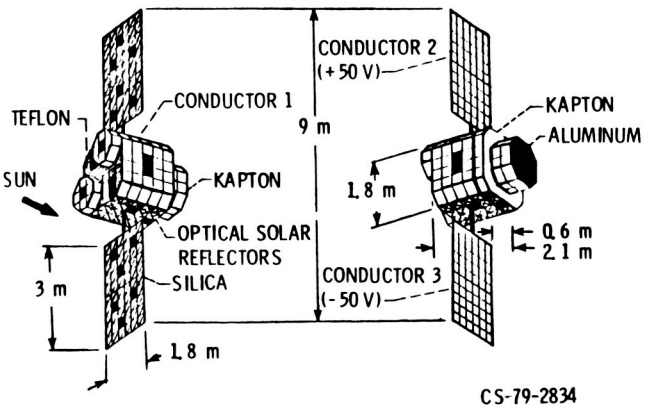

Figure 4. - Typical geosynchronous communications satellite.

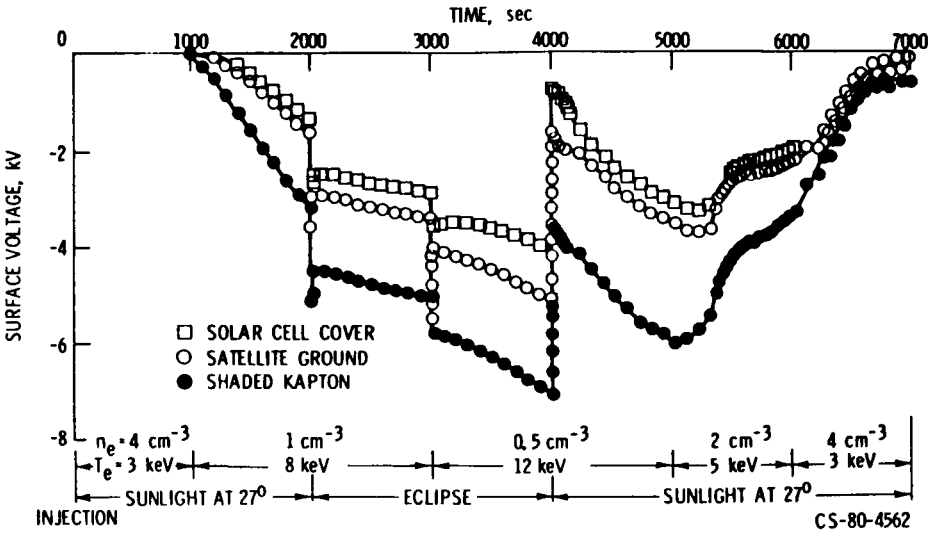

Figure 5. - Predicted potentials for substorm environment - three-axis-stabilized satellite.

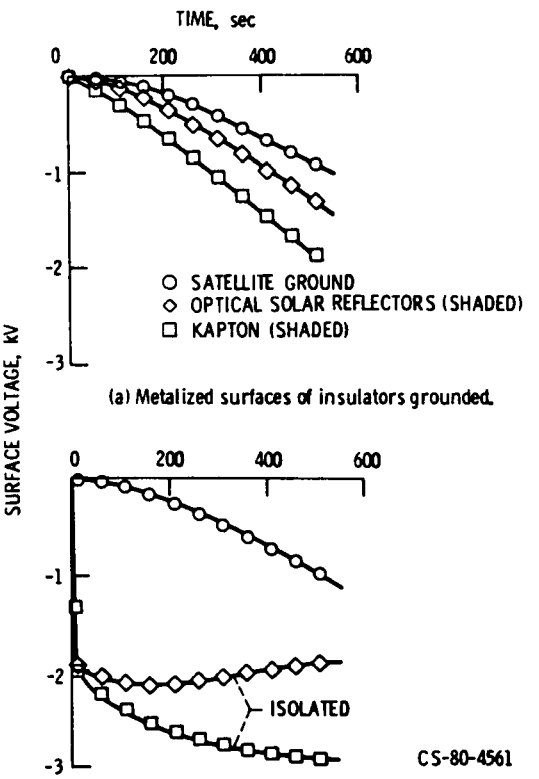

(a) Metalized surfaces of insulators grounded.

(b) Isolated insulators (capacity coupled to ground, $C = 10^{-12}$ F).

Figure 6. - Comparison of predicted surface voltages for grounded and isolated insulators. Environment: T_e = 8 keV; T_p = 16 keV; $n_e = n_p = 1$ cm^{-3}; sunlight at 27^0 incidence.

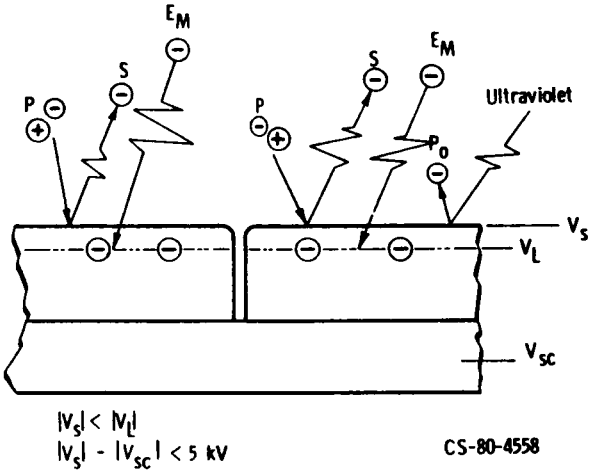

Figure 7. - Buried or trapped charge layers.

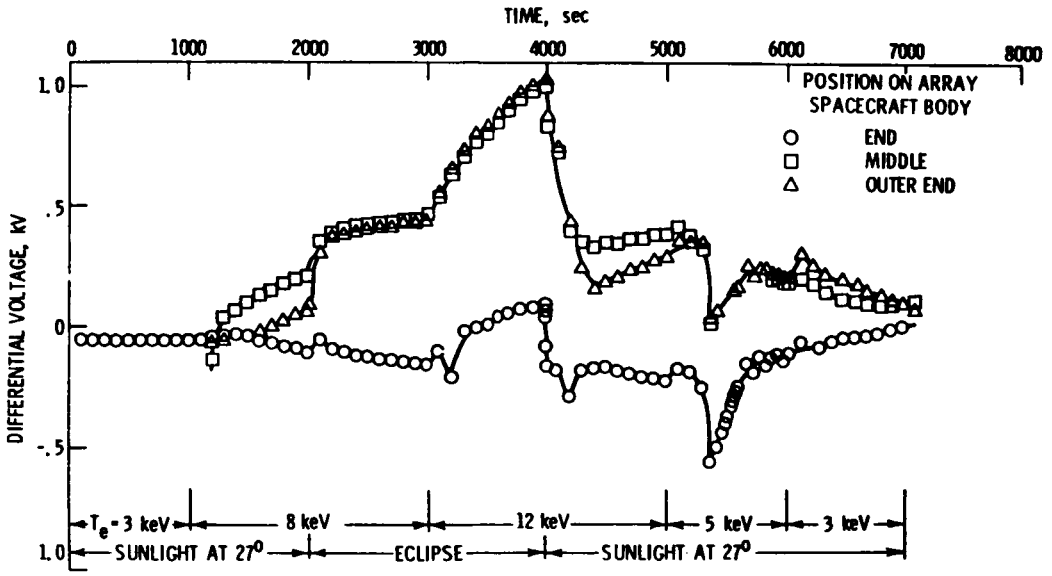

Figure 8. - Predicted differential voltages for positive bias solar array wing.